Use Of A New Developed Micro-Pulse-Like Reactor For The Kinetic Catalytic Measurements Of NO, NO_X Removal From Car Exhaust Gases On The New Catalyst (BZ Ag_2O, Al_2O_3-MoO_3- Ag_2O)

L. Al-Hamoud[(1)]; Y. Walid Bizreh[(2)] and M. Joubeh[(3)]

Department of Chemistry, Faculty of Sciences, Damascus University, Syria.

Received 22/01/2012
Accepted 28/05/2012

ABSTRACT

A new (ZB-Ag_2O, Al_2O_3-MoO_3 – Ag_2O) catalyst for dNO,dNOx and dCH has been prepared from silver oxide carried on a matrix of mixture from Syrian natural zeolite, Syrian bentonite and Al_2O_3-MoO_3–Ag_2O. Mineralogical studies were made to identical the components of the catalyst, montmorillonite and phylippsite and others were observed. The DTA diagrams indicated characteristic indothermal and exothermal reaction. The adsorption – desorption of N_2 measurements were carried out at -196°C. A slight decrease of surface area after having the catalyst been covered with Ag_2O. Catalytic experiments were conducted by means of a flow micro pulse-like reactor using the gas emitted from car exhaust. A maximal dNOx rate on the (ZB-Ag_2O, Al_2O_3-MoO_3 – Ag_2O) catalyst was observed at 185°C. The catalytic data make it possible to suggest a mechanism for the ongoing reactions.

Key Words: Micro-pulse-like method for dNO, dNOx and dCH from car exhaust gases, (ZB-Ag_2O, Al_2O_3- MoO_3 – Ag_2O) catalyst, Kinetic, Selective Catalytic Reduction (SCR), DTA & DTG Analysis, N_2 Adsorption – Desorption for (ZB-Ag_2O, Al_2O_3-MoO_3 – Ag_2O) catalyst.

[(1)]Student, [(2)] Superviser, [(3)] Associated superviser.

تطوير واستخدام جهاز حفزي شبه نبضوي تدفقي نصف صناعي للقياسات الحركية الحفزية لإزالة NO, NOx من غازات عوادم السيارات باستخدام حفاز جديد ($ZB\text{-}Ag_2O$, $Al_2O_3\text{-}MoO_3 - Ag_2O$)

لبنى الحمود[1] و يحيى وليد البزرة[2] و ملك الجبة[3]

قسم الكيمياء ــ كلية العلوم ــ جامعة دمشق ــ سورية

تاريخ الإيداع 2012/01/22
قبل للنشر في 2012/05/28

الملخص

حُضّر أول مرة حفاز ($ZB\text{-}Ag_2O$, $Al_2O_3\text{-}MoO_3 - Ag_2O$) لإزالة NO, NOx وCH على قاعدة مزيج من الزيوليت السوري الطبيعي (Z) والبنتونيت السوري الطبيعي (B) وأكسيد الفضة المحملين $Al_2O_3\text{-}MoO_3 - Ag_2O$. أُجريت الدراسة الكيميائية والفلزية للبنتونيت والزيوليت إذ تبين وجود مونتموريلونيت والفلز الزيوليتي من نوع "الفلبسيت". فضلاً عن ذلك أُجريت الدراسة الحرارية التفاضلية لعينات البنتونيت والزيوليت إذْ لوحظت أفعال ماصة وناشرة للحرارة. وقد درس امتزاز النتروجين في الدرجة -196° لكل من العينات، ولوحظ تناقص بسيط في المساحة السطحية بحسب BET ولانغمير لمزيج البنتونيت والزيوليت وحفاز الفضة عما كانت عليه في كل من البنتونيت والزيوليت ومزيج البنتونيت والزيوليت. وأُجريت أول مرة التجارب الحفزية باستخدام جهاز حفزي شبه نبضوي تدفقي نصف صناعي جديد يستخدم الغاز المنطلق من عوادم السيارات.ولوحظت أعلى نسبة إزالة NOx عند درجة حرارة 185°باستخدام الحفاز ($ZB\text{-}Ag_2O$, $Al_2O_3\text{-}MoO_3 - Ag_2O$). وقد اقْتُرحتْ آلية لتفاعل إزالة أكاسيد الآزوت بناءً على المعطيات التجريبية التي حصلنا عليها.

الكلمات المفتاحية: جهاز تدفقي ميكروي شبه نبضوي نصف صناعي لإزالة غازات NO – NOx – CH المنطلقة من عوادم السيارات، الحفاز ($ZB\text{-}Ag_2O$, $Al_2O_3\text{-}MoO_3 - Ag_2O$)، الحركية، الإرجاع الانتقائي الوساطي (SCR)، تحاليل DTG & DTA، امتزاز - مج النتروجين للحفاز ($ZB\text{-}Ag_2O$, $Al_2O_3\text{-}MoO_3 - Ag_2O$).

---

[1] طالبة دكتوراه، [2] مشرف، [3] مشرف مشارك.

1- Introduction

The selective catalytic reduction of NOx has attracted considerable interest as a method to control emission from car exhaust. The (Fe-BEA) catalyst [1] was studied for removal of NO and N_2O by NH_3 in the presence of O_2 .It was found that the removal of N_2O with iron sites was faster than the removal of NO with NH_3. A zirconium doped mesoporous silica as a support of Cobalt oxide [2] was used and tested in the selective catalytic reduction (SCR) of NO with ammonia in an excess of oxygen. These catalysts exhibited maximum conversion of NO (88%) at low temperature (200ºC). A highly dispersed Pt/Al_2O_3 catalyst[3] was used for the selective catalytic reduction on NOx using propene (HC-SCR). A linear correlation was found between the NO_x conversion in HC-SCR and the amount of $Pt_{surf,\ redox}$. Using non-zeolitic oxides and platinum group metal (PGM) catalysts has been critically reviewed. Alumina and silver-promoted alumina catalysts have been described in detail with particular emphasis on an analysis of the various reaction mechanisms [4]. SCR of nitrogen oxide (NO_x) by propane [5] was investigated in a micro reactor in the presence of H_2 on sol-gel prepared Ag/Al_2O_3 catalyst (0.5-5 wt. % Ag), attaining considerable activity within a wide temperature window (470-825 K). SCR of NO with CH4 was studied over ZSM-5, MOR, FER and BEA zeolite-based cobalt (Co) and palladium (Pd) catalysts in the presence of oxygen and water. The most active catalysts, is that was based on MOR and ZSM-5 [6]. In [7] Copper proved to be the best metal cation for lean-NO_x catalysts with the optimum level of exchange at 29-42 %. The optimized, fresh Cu/SUZ-4 catalyst achieved 70-80 % of NO/NOx conversion activity over a wide range of temperature from 350 to 600ºC with the maximum conversion temperature at 450ºC. The catalyst $Cu\text{-}Al_2O_3$was studied by using linear and branched alkanes with different carbon numbers and they found that the structure of hydrocarbon had no influence on the selectivity [8]. Some works have focused on the effect of carbon number on de-NOx activity of $Ag\text{-}Al_2O_3$ catalyst [9]. Ag/Al_2O_3, Ag-ZSM5, Ag-HY catalysts and all three catalysts showed high selectivity to N_2 (around 95%) through several characterization, it was concluded that silver was present in the form of Ag_2O clusters, but not in metallic form for three catalysts [10]. In [11] it was shown that the Pt---Ir---Rh/MFI zeolite catalyst showed higher performance and durability than the current Pt---Rh supported on alumina and ceria catalyst. Whereas in [12] it was observed that $Ag\text{-}Al_2O_3$ had higher NO conversion to N_2

and selectivity than alumina-supported Pt and Cu-ZSM-5 catalysts for the selective reduction of NO by *n*-octane and *i*-octane.

2- Objective

the main goal of the present study is to prepare a new catalyst for d-NOx emitted along with car exhaust gases from silver and molybdenum oxides supported on a matrix from Syrian natural zeolite of the "Sys" deposit (southern part of Syria), Syrian bentonite (Aleppo area) and alumina supported silver oxide and a study of the catalytic and surface properties.

3- Chemicals

a. Silver nitrate (Pure).
b. Ammonium molybdat (MAY & BAKER)
c. Aluminum oxide (Alumina Oxide 90, Merck).
d. Syrian zeolite (Z).
e. Syrian bentonite (B).

4- Equipments used in the present study:

a. X-Ray Fluorescence X.R.F. (Seouential ARL 8410).
b. X-Ray diffraction (P W 1830 PHILIS).
c. Differential Thermal Analysis D.T.A. device (DTG-60H SHIMADZU).
d. The Surface Area device (Micromeritics Gemini 3).
e. GAS Analyzer (Kane).
f. Compressor
g. Furnace (Carbolite).
h. The new developed micro pulse -like flow catalytic pilot plant.

5- Experimental

Preparation of the (ZB-Ag_2O, Al_2O_3-MoO_3-Ag_2O) catalyst: it was prepared as the following stages:

Stage A: Preparation of the alumina supported metal oxide:

1A- 6.66 gr. of ammonium molybdate were dissolved in 88.3 ml of hot distillated water, 46.92gr. of silver nitrate were added and dissolved in the solution (solution I).

2A- Solution (I) was impregnated with 166.78 gr. of alumina to form a paste, about 50 ml of distillated water were added and mixed with the paste, the paste was put to dry in the shade.

3A- The dried product was heated at 110°C for 4 hours.

4A- The outcomming mass was heated at 550°C in the oven for 5 hours.

Stage B: impregnation of Syrian bentonite (B) and Syrian zeolite (Z) with silver nitrate solution:

1B- 400 gr. of Syrian bentonite (B) "Aleppo area" were impregnated with 400 ml of 0.075 N silver nitrate solution.

2B- 393 gr. of Syrian bentonite (B) "Aleppo area" were impregnated with 393 ml of 0.075 N silver nitrate solution.

3B- 333 gr. of natural Syrian zeolite (Z) from "Sis deposit" (Southern part of Syria) was mixed with 111 ml of 0.6 N silver nitrate solution.

Stage C:

1C- The produced powder of stage A was divided into three parts, each of them was added to each one of the masses 1B, 2B, 3B of stage B respectively.

Fig. 1. Fractions of silver and molybdenum catalyst ZB-Ag_2O, Al_2O_3-MoO_3- Ag_2O

2C- The paste was formed in cylinders of 5 cm. length and internal diameter of 2 mm, and as thin as 3mm

3C- The received tubes were dried at room temperature in shade for 7 days.

4C- The dried tubes were heated in the "Carbolite" oven at 550°C for 5 hours. In order to decompose all the nitrate residual.

5C- The prepared catalyst was used after cooling in the same oven till the next day (Fig. 1).The resulting cylinders were turned into pieces of 1-1.5 cm length.

6- Results in respect of Syrian zeolite "sys deposit" and Syrian bentonite:

6-1: Chemical analysis:

6-1-1: The Chemical analysis of the Syrian zeolite: the following table shows the results of the analysis by using of X. R. F.:

Table 1. Results of the analysis of the Syrian zeolite

Oxide	TiO_2	K_2O	Na_2O	MgO	CaO	Fe_2O_3	Al_2O_3	SiO_2
Percentage %	1.81	0.60	0.28	4.50	15.33	9.29	11.37	37.08

Oxide	L.O.I	Cl^-	Cr_2O_3	P_2O_5	SO_3	Mn_2O_3
Percentage %	18.55	0.05	0.015	0.50	<0.02	0.111

6-1-2: The Chemical analysis of the Syrian bentonite: the following table shows the results of the analysis by using of X. R. F.:

Table 2. Results of the analysis of the Syrian bentonite

Oxide	TiO_2	K_2O	Na_2O	MgO	CaO	Fe_2O_3	Al_2O_3	SiO_2
Percentage %	1.21	0.46	0.11	5.77	6.76	8.30	11.85	46.76

Oxide	L.O.I	Cl^-	Cr_2O_3	P_2O_5	SO_3	Mn_2O_3
Percentage %	18.40	0.08	0.030	0.13	<0.02	0.107

6-2: X. R. D. analysis:

6-2-1: X. R. D. analysis of the Syrian zeolite: the Fig. 2 shows the analysis of the Syrian zeolite which consists of calcite, **philpsite** and montmorillonite

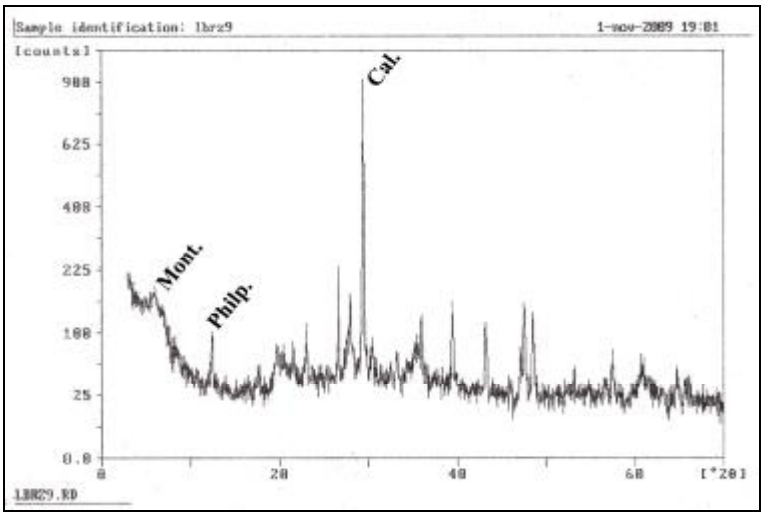

Fig. 2. X. R. D. analysis of the Syrian zeolite

6-2-2: X. R. D. analysis of the Syrian bentonite: the Fig. 3 shows the analysis of the Syrian bentonite which consists of quartz, dolomite, calcite, **palegorskite,** kaolinite and montmorillonite

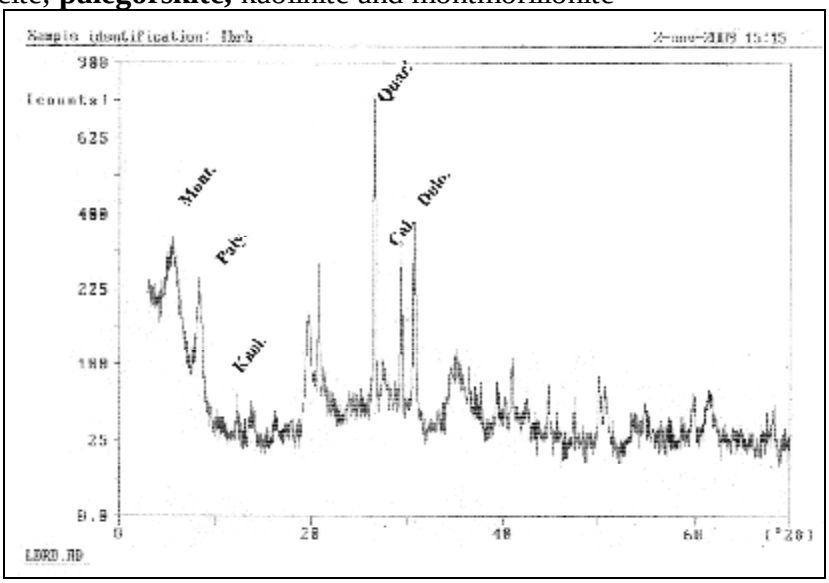

Fig. 3. X. R. D. analysis of the Syrian bentonite

6-3: Thermal study:

6-3-1: D. T. A. analysis of the Syrian zeolite: Fig. 4 showing the D. T. A. analysis of the Syrian zeolite which indicate an endo-thermal action at 94.85°C – 171.26°C and 754.82°C and exo-thermal action at 778.88°C and 838.92°C.

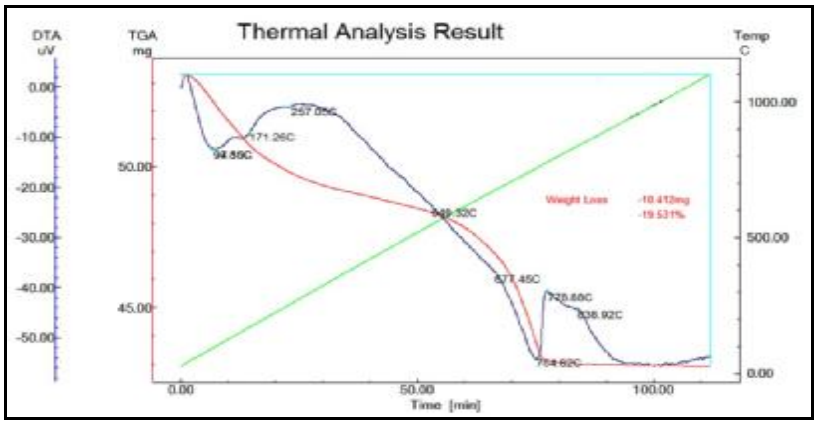

Fig. 4. D. T. A. analysis of the Syrian zeolite

6-3-2: D. T. A. analysis of the Syrian bentonite: Fig. 5 showing the D. T. A. analysis of the Syrian bentonite which indicates an endo-thermal action at 107.34°C – 224.36°C and 747.25°C and exo-thermal action at 764.15°C.

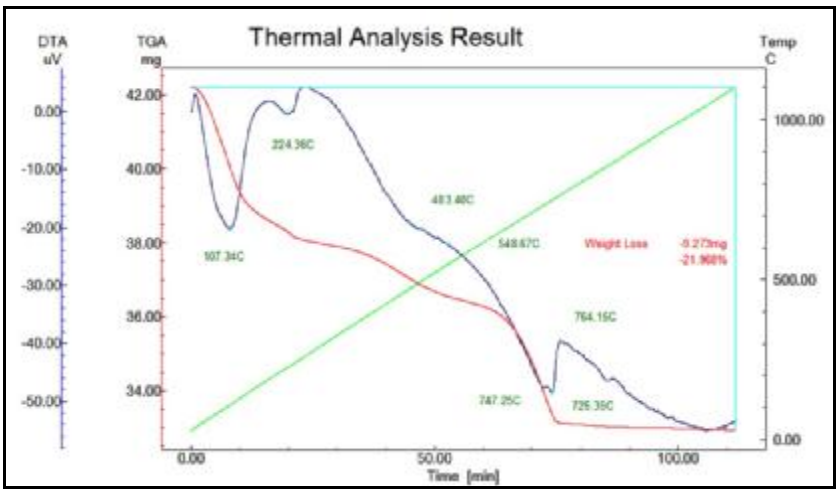

Fig. 5. D. T. A. analysis of the Syrian bentonite

6-4: N_2 adsorption – desorption measurements: surface area of the catalyst was measured by means of Micromeritics Gemini 3 device data of which are listed in table (3).

Table 3. Data surface properties for bentonite (B), zeolite (Z), the combined bentonite and zeolite (ZB) and the Syrian sliver catalyst ZB-Ag_2O, Al_2O_3-MoO_3- Ag_2O

ZB-Ag_2O, Al_2O_3-MoO_3- Ag_2O	Combined ZB	Zeolite (Z)	Bentonite (B)	Surface parameter
34.4682	52.6014	49.3041	51.7946	**Surface area (m^2/g. BET)**
54.4739	81.9353	76.2058	82.1938	**Surface area (m^2/g. Langmure)**
1.3130	9.5036	13.3858	0.4878	**Micropore area m^2/g.**
33.1553	43.0978	35.9183	51.3067	**External surface area m^2/g.**
0.00046	0.0047	0.0069	0.000017	**Micropore volume cm^3/g.**
0.0489	0.0631	0.0515	0.0620	**Overall micropore volume a at certain value of P/P_0 cm^3/gr.**
56.7551	48.0197	41.7892	47.8927	**Average pore diameter A^0**

Table (3) indicates a sharp decrease of surface area in the direction bentonite-zeolite- ZB-Ag_2O, Al_2O_3-MoO_3-Ag_2O, whereas the pore diameter average increased in the direction zeolite (Z)- zeolite bentonite (ZB) - ZB-Ag_2O, Al_2O_3-MoO_3-Ag_2O. Plots for N_2 adsorption the ZB-Ag_2O, Al_2O_3-MoO_3- Ag_2O catalyst and pore distribution are shown in Figs (6,7). The adsorption desorption isotherm may be classified as type B of De Boer classification of capillary condensation hysteresis loops [13].

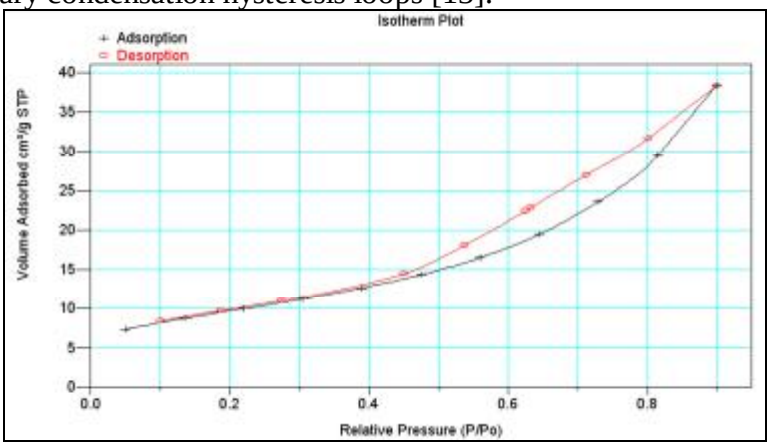

Fig. 6. N_2 adsorption–desorption isotherms for the catalyst ZB-Ag_2O, Al_2O_3-MoO_3- Ag_2O

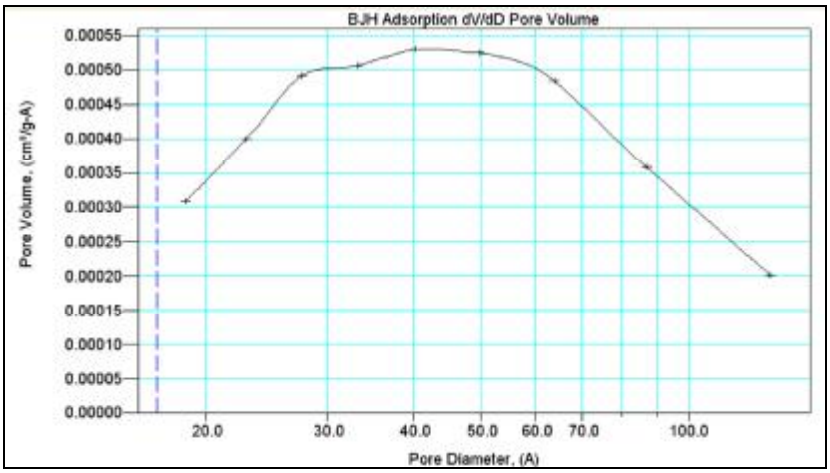

Fig. 7. Pore volume distribution as a function of pore diameters in case of N_2 adsorption for the catalyst ZB-Ag_2O, Al_2O_3-MoO_3- Ag_2O.

6-5:Results of the catalytic study:

6-5-1: Dependence of conversion rate on time at different temperatures and space velocities: data listed in the following plots 8-9-10 and table 4 represent the dependence of the de-NO, de-NOx and de-CH conversion rate on time and flow rate at temperatures 135°C, 150°C and 185°C, respectively. The results and curves show increasing conversion rates, to reach a stationary state and consequently a constant conversion rate in most cases.

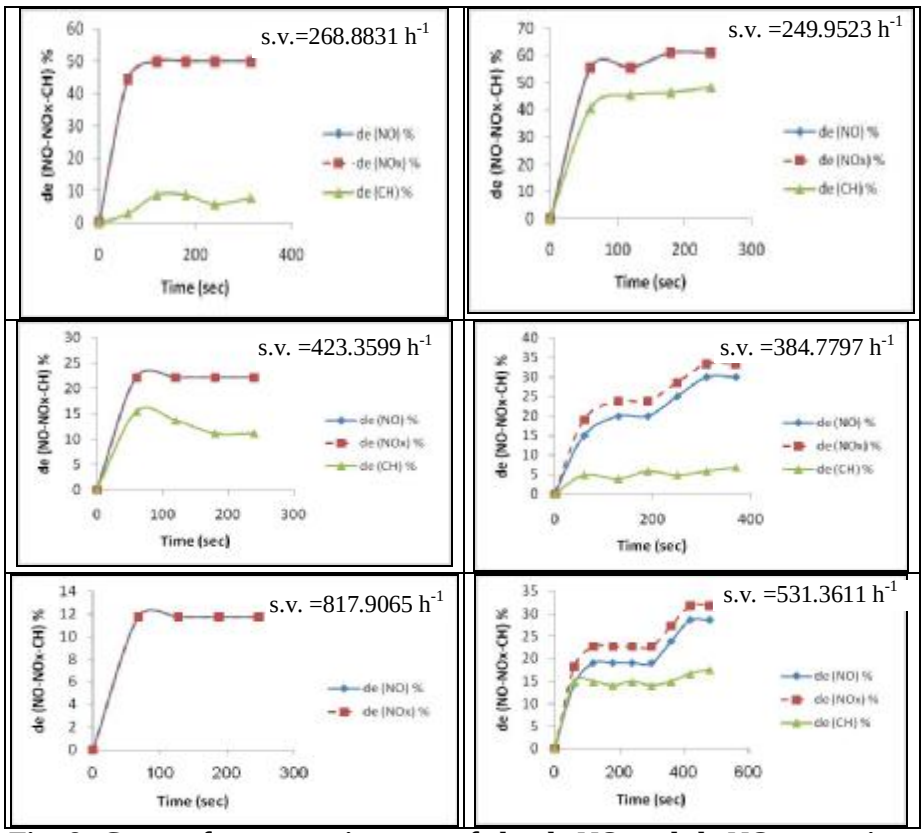

Fig. 8. Curves for conversion rate of the de-NO and de-NOx, reactions at 135°C and different space velocities (s.v.) for ZB-Ag_2O, Al_2O_3-MoO_3- Ag_2O

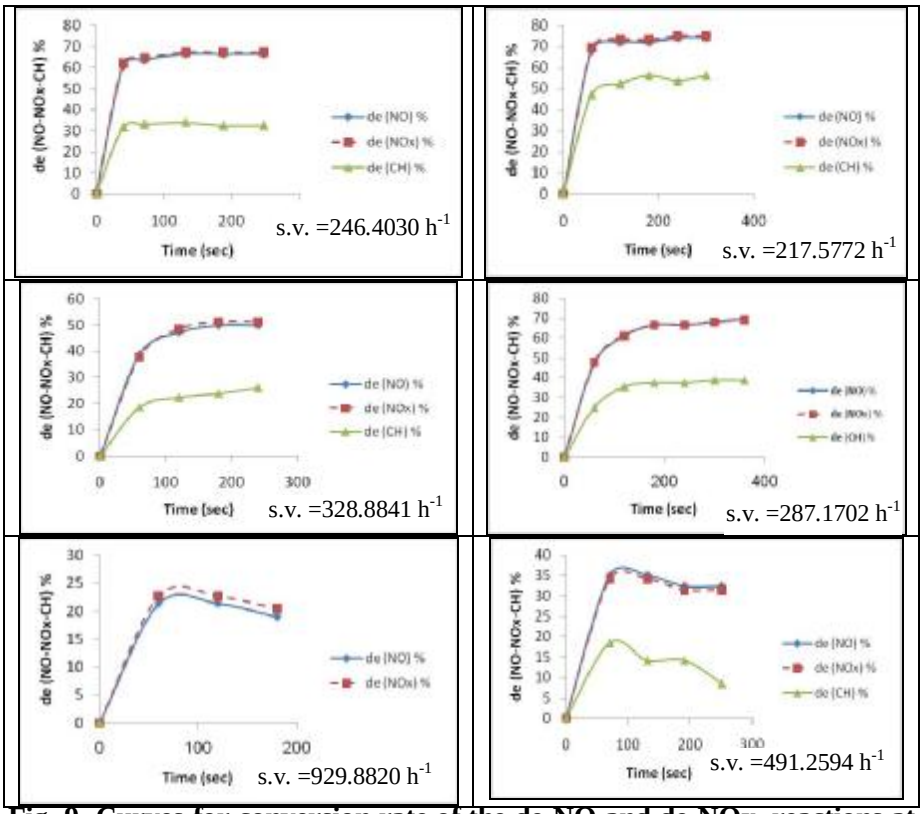

Fig. 9. Curves for conversion rate of the de-NO and de-NOx, reactions at 150°C and different space velocities (s.v.) for ZB-Ag_2O, Al_2O_3-MoO_3- Ag_2O.

Table 4. Results and curves for conversion rate of the de-NO, de-NOx and de-CH reactions at 185°C and different space velocities for ZB-Ag_2O, Al_2O_3-MoO_3- Ag_2O

270.2766 h^{-1}		Space Velocity	Syrian Molybdenum and Silver catalyst	222.2170 h^{-1}		Space Velocity	Syrian Molybdenum and Silver catalyst
°185		Temperature		°185		Temperature	
Removal of NOx %	Removal of NO %	Removal of CH %	Time S	Removal of NOx %	Removal of NO %	Removal of CH %	Time S
0.0000	0.0000	0.0000	0.0000	0.0000	0.0000	0.0000	0.0000
69.0476	67.5000	20.8791	62	73.0770	72.0000	74.4440	167
76.1905	75.0000	29.6703	122	76.9230	76.0000	77.7780	227
78.5714	77.5000	40.6593	182	80.7690	80.0000	78.8890	287
78.5714	77.5000	45.0549	242	82.6920	82.0000	78.8890	347

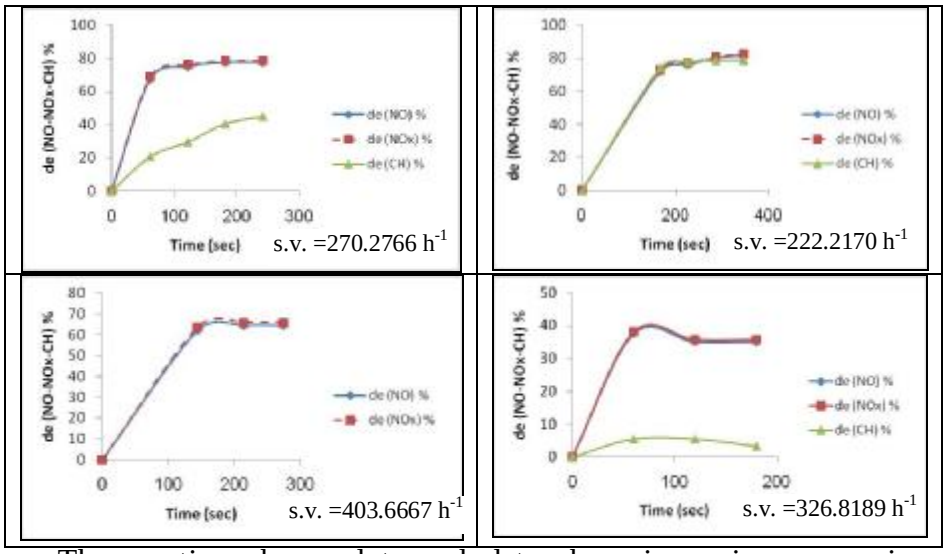

The mention above plots and data show increasing conversion rates, to reach a stationary state and consequently a constant conversion rate in most cases.

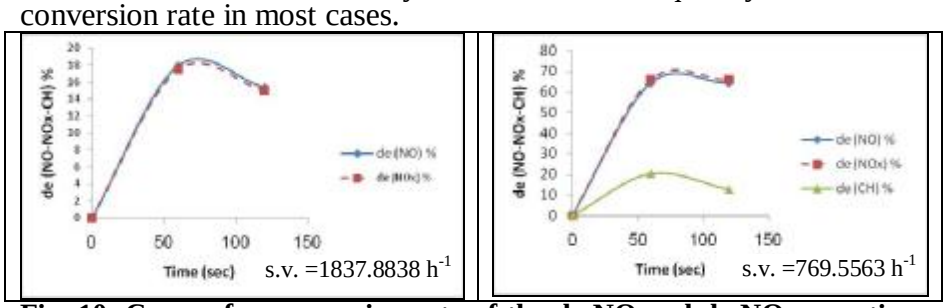

Fig. 10. Curves for conversion rate of the de-NO and de-NOx, reactions at 185°C and different space velocities (s.v.) for ZB-Ag_2O, Al_2O_3-MoO_3- Ag_2O

6-5-2: Dependence of the de-NO, de-NOx and de-CH reaction on temperature at close space velocities: for the Syrian sliver catalyst ZB-Ag_2O, Al_2O_3-MoO_3-Ag_2O at the following space velocities: 268.8831 - 287.1702 - 270.2766 h^{-1}

Table 5. Results of de-NO, de-NOx and de-CH as a function of temperatures for ZB-Ag_2O, Al_2O_3-MoO_3- Ag_2O

Space Velocity h^{-1}	de (NOx) %	de (NO) %	de (CH) %	Temperature C°
268.8831	50	50	7	**135**
287.1702	69	69	38	**150**
270.2766	78	77	45	**185**

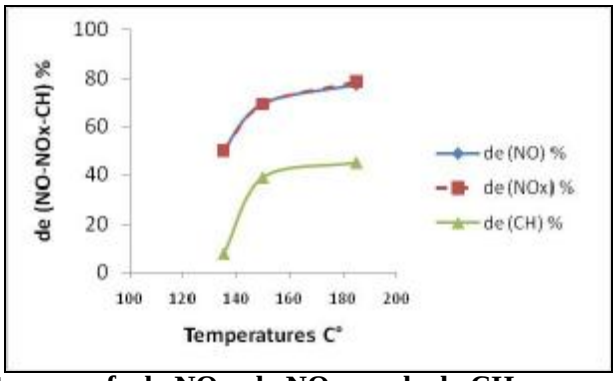

Fig. 11. Curves of de-NO, de-NOx and de-CH as a function of temperatures for ZB-Ag_2O, Al_2O_3-MoO_3- Ag_2O

Results are represented in Table 5 and Fig. 11 and indicate higher conversions for de-NO, de-NOx and de-CH at 185°C, whereas lower conversion rate was taking place at 135°C. Those results are in accord with data in references [14-18].

6-5-3: Dependence of conversion rate on flow rate for car exhaust gas at different temperatures was determined by means of micro pulse flow method that already was used for isomerization and cracking of light hydrocarbons [19-21] and it has been modified and suggested **for the first time in our work.**

6-5-3-1:The modified Theoretical fitting of the innovated development pilot plant for kinetics of catalytic removal of NO, NOx and CH pollutants from gases emitted from car exhausts can be summarized as follows:

When a volume of gas with the reacting material passes through the catalytic reactor containing dm g. of the catalyst at an instant, n moles of the reactant will be distributed between the gas phase of the volume v_g dm where v_g is the volume of the gas space at the sector of the catalytic reactor that contains 1g. catalyst, and the adsorbed phase where the reaction takes place.

Assuming that P_A is the partial pressure of the reactant, and K_A is the adsorption equilibrium constant for 1 g. of the catalyst, then we may write the total mole number (n) as the following:

$$n = \frac{P_A v_g \, dm}{RT} + K_A P_A \, dm \qquad (1)$$

The adsorption equilibrium constant K_A is related with the adsorbed volume of the reactant gas by one gram of the catalyst v_A with the equation [22]:

$$K_A = \frac{v_A}{RT} \qquad (2)$$

and the value of n will be

$$n = P_A(v_g + v_A)\,\frac{dm}{RT} \qquad (3)$$

$$P_A dm = \frac{nRT}{v_g + v_A}$$

Since the surface reaction controls the reaction rate and k (s^{-1}) is the first order real rate constant of the surface reaction, the rate of reaction of the adsorbed reactant in the related section of catalyst is:

$$-\frac{dn}{dt} = k\,K_A P_A\,dm$$

$$= \frac{k\,K_A\,n\,RT}{v_g + v_A} \qquad (4)$$

Rearranging (4) we get the following equation:

$$-\frac{dn}{n} = \frac{kK_A RT}{v_g + v_A}dt \qquad (5)$$

and the conversion rate is independent of the pressure.

If n in equation (4) is replaced by the whole reacting moles in the space of reaction, then the integration of equation (5) will lead to:

$$\ln\frac{1}{1-X} = \frac{RTkK_A}{v_g + v_A}t \qquad (6)$$

Where X is the conversion rate and (t) is the time of stay of the reacting moles on the surface of the catalyst

When F (ml s^{-1}) is the flow rate of the gases mixture in the reacting molecules at the reactor temperature and the mean pressure. The time of stay (t) of the reactant in the reacting space is

$$t = (v_g + v_A)\frac{m}{F} \qquad (7)$$

where m is the whole mass of the catalyst.

Substituting (7) in the equation (6) is

$$\ln\frac{1}{1-X} = \frac{RTkK_A}{v_g + v_A}\,(v_g + v_A)\,\frac{m}{F}$$

$$\ln\frac{1}{1-X}=\frac{RTkK_Am}{F} \qquad (8)$$

Replacing K_A in equation (8) with its value from equation (2) we receive:

$$\ln\frac{1}{1-X}=\frac{RTk}{F}\frac{v_Am}{RT}=\frac{v_Am}{F}k=\frac{V_Ak}{F}$$

where the V_A is the adsorbed volume of the reactant on the surface of the catalyst ($V_A = v_A$ m)

The flow rate (F) in an experiment is measured **at room temperature** and mean pressure and corrected to zero C° to become:

$$F_0=\frac{273F}{T} \qquad (9)$$

If (9) is taken into account, the equation (8) will have the form:

$$\ln\frac{1}{1-X}=\frac{RTm}{\frac{F_0T}{273}}kK_A=\frac{R273m}{F_0}kK_A$$

$$\frac{1}{m}\ln\frac{1}{1-X}=(273RkK_A)\frac{1}{F_0} \qquad (10)$$

The apparent activation energy of the considered reaction can be determined from

$$\ln\left(\frac{1}{m}\ln\frac{1}{1-X}\right)=f\left(\frac{1}{T}\right) \qquad (11)$$

Where: m: is the mass of the catalyst, X:is the conversion rate for the de-NO, de- NOx and de-CH reaction, K_A: is the adsorption equilibrium constant, k: is the real rate constant as for the NO, NOx and CH reagents.

A special new pilot plant corresponding to the above theoretical (Figs 12,13) has been constructed in our laboratory to fit the investigated issue.

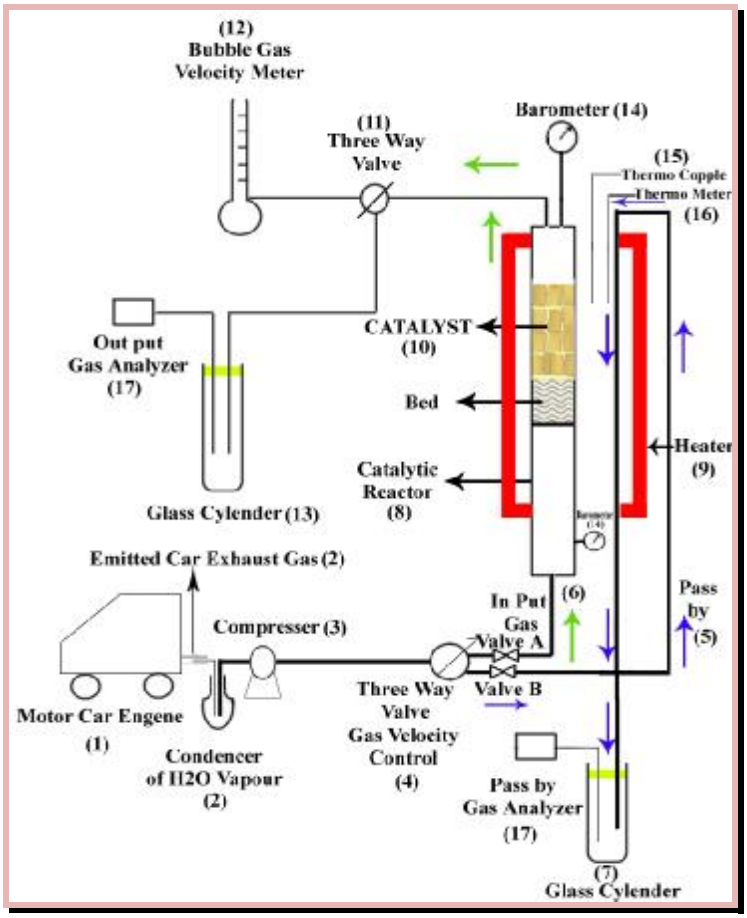

Fig. (12) represents the constituent of the new devise as follows:

1- A motor car with internal combustion engine.
2- Gases emitted from car exhaust passing through a condenser of water vapors.
3- Car exhaust gas compressor attached to a gas regulator.
4- Three way gas velocity controlling valve.
5- Pass by flow gas tube through the heating system with a valve B.
6- Flow gas tube with valve A for the reacting gas in the catalytic reactor.
7- A glass cylinder for the passing by gas analysis.
8- Catalytic pilot plant reactor.
9- Electric heater.
10- The catalyst layer on a bed.
11- Three way valve.
12- Velocity foam bubble gas meter.
13- A glass cylinder for the out coming gas from the reactor.
14- Barometer.
15- Thermo couple connected to a thermostat.
16- Thermometer for relatively high temperatures.
17- Gas Analyzer (detector)

A photograph of the related constructed rig is shown in Fig. 13

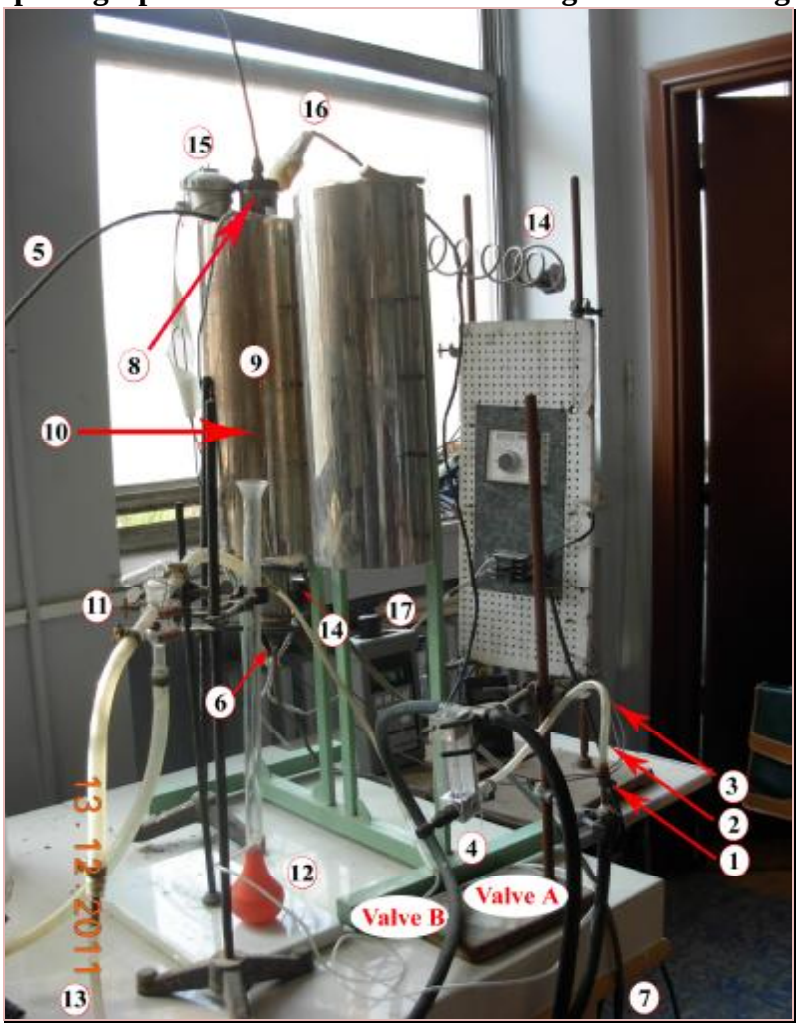

Fig. 13. A photograph of the related constructed rig.

6-5-3-2 Method of Experiment:

1- Inserting 100 g. of the catalyst (10) were inserted into the reactor (8).
2- Transmitting the car exhaust gas was from the vehicle (1) via rubber tubes (2) and a water vapor condenser (2) to a gas compressor (3).

3- The reacting gas passes from the compressor (3) to a three way gas velocity controlling valve (4).
4- In order to start the measurements valve (B) is closed simultaneously with valve (A) being opened to make the car exhaust gas pass through to the catalytic reactor (8) heated by the oven (9). The reacted with the contact mass gas (10) move through the three way valve (11) to the bubble gas velocity meter (12) for the output gas.
5- Valve (A) is closed and valve (B) is opened to make the gas flow from valve (B) through the tube (5) via heater (9) passing by the catalyst to be analyzed after being catalyzed in a glass cylinder (7), the result of analyses provide the structure of the passby gas exhaust heated to the same temperature of the heated catalyst in the reactor.
6- The next step is to open valve (A) and shut off the valve (B) at the same moment in order to make three minutes gas pulse pass through in the reactor (8) and get reacted in the catalyst layer (10). The resulting gas and products of the catalytic reaction pass to the three way valve (11) to be collected in the glass cylinder (13) and analyzed by means of the KANE GAS ANALZER.
7- Step (5) is to be repeated to make sure that the structure of the initial reacting car exhaust gas before the catalytic measurements is identical to the structure of the initial gas after measuring the catalytic activity at the same temperature and mean pressure.

6-5-3-3: Results

Data for measurement at 135°C, 150°C and 185°C are represented in the following plots:

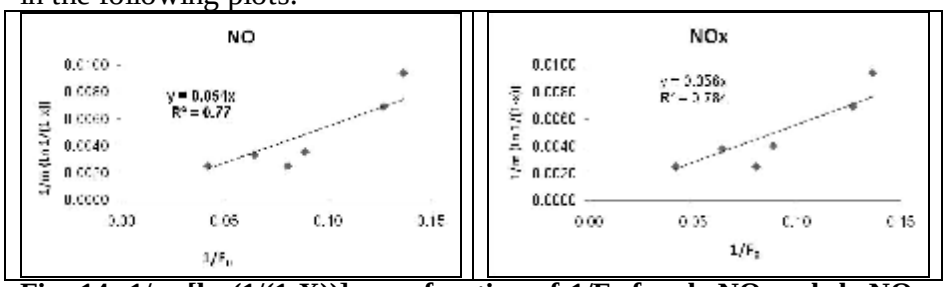

Fig. 14. 1/m [ln (1/(1-X))] as a function of $1/F_0$ for de-NO and de-NOx and catalytic reaction at 135°C for ZB-Ag_2O, Al_2O_3-MoO_3-Ag_2O

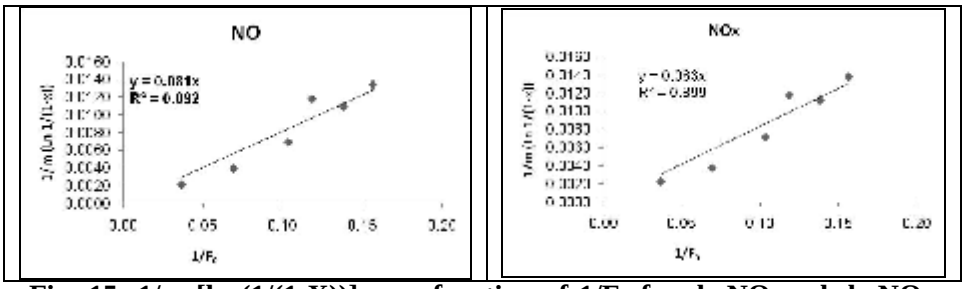

Fig. 15. 1/m [ln (1/(1-X))] as a function of $1/F_0$ for de-NO and de-NOx catalytic reaction at 150°C for ZB-Ag_2O, Al_2O_3-MoO_3- Ag_2O

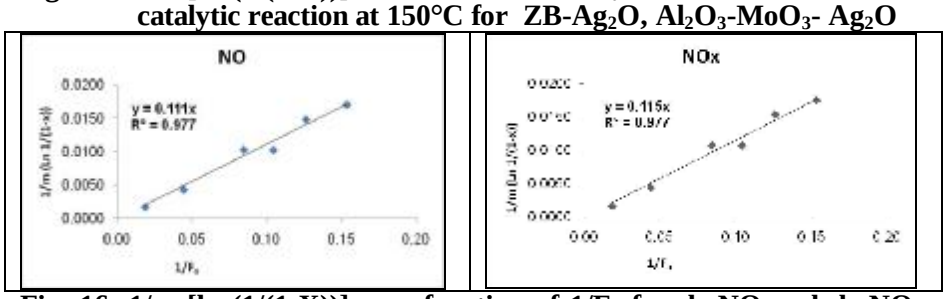

Fig. 16. 1/m [ln (1/(1-X))] as a function of $1/F_0$ for de-NO and de-NOx catalytic reaction at 185°C for ZB-Ag_2O, Al_2O_3-MoO_3- Ag_2O.

Plots of Figures 14, 15, 16 show good agreement with the equation (10) indicating a pseudo first order reaction as for de-NO, de-NOx conversion at 135°, 150°and 185°C respectively.

Values of $K_A k$ by means of the equation (10) are listed in table(6):

Table 6. Values of $K_A k$ by means of the equation (10)

Temperatures C°	de-NO	de-NOx
	$K_A k$ m mol/ g. s atm	$K_A k$ m mol/ g. s atm
135°	0.00241	0.0025
150°	0.00361	0.0037
185°	0.00495	0.00513

Those results are generally in accordance to the results obtained in [23] where a fractional order for de-NO, as observed for a catalyst is different from our catalysts.

6-5-4: Calculation of activation energy: The activation energy were calculated by means of equation: Log {1/m [Ln (1/(1-x))]}= f (1/T)

Activation energy = slope 2.303 R where R is universal gases constant

The activation energy was calculated with data of 135°C–150°C-185°C

- **Group A**: Activation energy at flow rates of 7.3288-7.2247-6.5156 cm^3/s

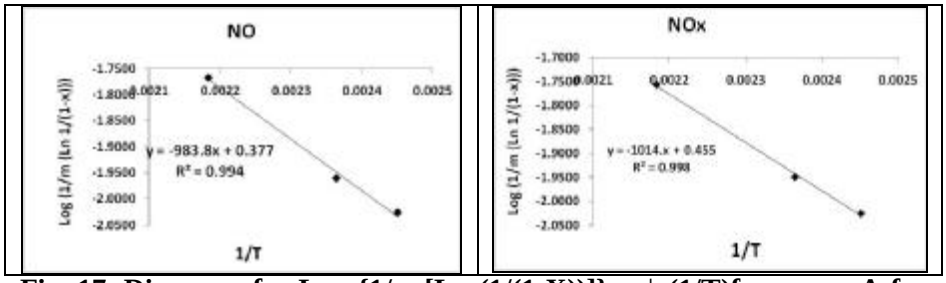

Fig. 17. Diagrams for Log {1/m [Ln (1/(1-X))]} = ¦ (1/T)for group A for ZB-Ag_2O, Al_2O_3-MoO_3- Ag_2O

The calculated apparent activation energy for group A are 18.8 and 19.4 (K J) /mol for NO and NOx respectively.

- **Group B**: Activation energy at flow rates of 7.8839- 8.4201-7.9247 cm^3/s

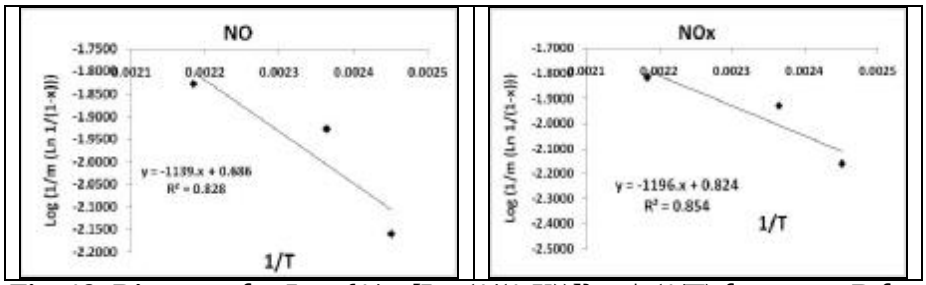

Fig. 18. Diagrams for Log {1/m [Ln (1/(1-X))]} = ¦ (1/T) for group B for ZB-Ag_2O, Al_2O_3-MoO_3- Ag_2O

The calculated apparent activation energy for group B are 21.80 and 22.89 (K J) /mol for NO and NOx respectively.

The received values of activation energy are in accordance with those obtained in [5].

The decreasing catalytic activity with the increased temperature can be attributed to decreasing **adsorption of NO, NO_X** which is presumed to be the rate limiting step, that is, the suggested mechanism of the catalytic de-NO, de-NOx may be as follows [24, 25]:

$_*$ as + NO → NO_{Ads}

NO_{Ads} + NO_g → N_2O + O_{Ads}

2 NO_{Ads} → N_2 + 2 O_{Ads}

2 O_{Ads} → O_{2g} + 2$_*$ as

As for the catalytic de-CH the related mechanism is:

C_xH_y + zO_{Ads} → $(C_xH_yO_z)$ $_{\text{Ads Intermediate}}$ → m CO_2 + n H_2O

This mechanism is based on the results of a single experiment, that is, the absence of any reaction in the pass by of the same car exhaust gas flowing through tube (6) in the oven at identical temperatures and flow rates (Figs. 12,13). This conclusion may be not common for all different O.N. gasoline fuels.

7- **A comparative study was conducted between our catalyst ZB-Ag_2O, Al_2O_3-MoO_3-Ag_2O and a honey comb structure commercial catalyst manufactured for use in gasoline vehicles:** The experimental measurement were carried out with our developed rig in almost close conditions. Results for NO, NOx removal catalyzed by our catalysts **ZB-Ag_2O, Al_2O_3-MoO_3- Ag_2O** and a commercial catalyst are listed in (Table 7).

Table 7. de-No, de-NOx rates of commercial catalyst compared with those of our Syrian catalyst.

Commercial Catalyst		ZB-Ag_2O, Al_2O_3-MoO_3- Ag_2O		Space Velocity cm^3/s	Temperature C°
de-NOx %	de-NO %	de-NOx %	de-NO %		
% 80	% 80	-	-	421.0	°175
-	-	% 65.9	% 64	403.6	°185

The exceeded conversion rate value related to the commercial catalyst may be attributed to its chemical and honey comb structure.

8- Conclusions

1- A maximum conversion rate for de-NO_X, de-NO and de-CH reaction has been reached at 185°C and close flow rates for the catalyst ZB-Ag_2O, Al_2O_3-MoO_3- Ag_2O

2- A new pilot-plant corresponding to the theoretical principle of a micro-pulse reactor has been developed for measuring the catalytic activity and kinetics of NO_X catalytic removal from emitted car exhaust gases

3- The resulting de-NO_X, de-NO kinetic data for the catalyst ZB-Ag_2O, Al_2O_3-MoO_3- Ag_2O have been proved to be in accordance with the derived kinetic first order equation at 135°C,150°C and 185°C.

4- The apparent constants and activation energies were calculated by use of data obtained by means our new developed pilot plant (rig).

REFERENCES

[1] Coq, B., Mauvezin, M., Delahay, G., Butet and J. B., Kieger, S., 2000. The simultaneous catalytic reduction of NO and N_2O by NH_3 using an Fe-zeolite-beta catalyst. *Appl. Catal., B Vol. 27 pp. 193-198.*

[2] Moreno-Tost, R., Santamaria-Gonzalez, J., Maireles-Torres, P., Rodriguez-Castellon, E. and Jimenez-Lopez, A., 2002. Cobalt supported on zirconium doped mesoporous silica: a selective catalyst for reduction of NO with ammonia at low temperatures. *Appl. Catal. B, vol. 38 pp. 51-60.*

[3] Vaccaro, A. R., Mul, G., Perez-Ramirez, J. and Moulijn, J. A., 2003. On the activation of Pt/Al_2O_3 catalysts in HC-SCR by sintering: determination of redox-active sites using Multitrack. *Appl. Catal. B, Vol. 46 pp. 687-702.*

[4] Burch, R., Breen, J. P., and Meunier, F. C., 2002. A review of the selective reduction of NOx with hydrocarbons under lean-burn conditions with non-zeolitic oxide and Platinum group metal catalysts. *Appl. Catal. B, Vol. 39 pp. 283-303.*

[5] Richter, M., Bentrup, U., Eckelt, R., Schneider, M., Pohl, M. M. and Fricke, R., 2004. The effect of hydrogen on the selective catalytic reduction of NO in excess Oxygen over Ag/Al_2O_3. *Appl. Catal. B, Vol. 51 pp. 261-274.*

[6] Pieterse, J. A. Z., Brink, R. W., Booneveld, S. and Bruijn, F. A., 2003. Influence of Zeolite structure on the activity and durability of Co-Pd-Zeolite catalyst in the reduction of NOx with methane. *Appl. Catal. B, Vol. 46 pp. 239-250.*

[7] Subbiah, A., Cho, B. K., Blint, R. J., Gujar, A., Price, G. L. and Yie, J. E., 2003. NOx reduction over metal-ion exchanged novel zeolite under lean conditions: activity and hydrothermal stability. *Appl. Catal. B, Vol. 42 pp. 155-178.*

[8] Shibata, J., Shimizu, K. I., Satsuma, A. and Hattori,T., 2002. Influence of hydrocarbon structure on selective catalytic reduction of NO by hydrocarbon over Cu- Al_2O_3. *Appl. Catal. B, Vol. 37 pp. 197-204.*

[9] Schimizu, K., Shibata, J., Satsuma, A. and Hattori, T., 2001. Mechanistic causes of the hydrocarbon effect on the activity of $Ag–Al_2O_3$ catalyst for the selective reduction of NO. *Phys. Chem. Chem. Phys., V. 3, pp. 880-884.*

[10] Furusawa, T., Seshan, K., Lercher, J. A., Lefferts, L. and Aika, K., 2002. Selective reduction of NO to N2 in the presence of oxygen over supported silver catalysts. *Appl. Catal. B, Vol. 37 pp. 205-216.*

[11] Takami, A., Takemoto, T., Lwakuni, H., Yamada, K., Shigetsu, M. and Komatsu, K., 1997. Zeolite-supported precious metal catalysts for NOx reduction in lean burn engine exhaust. *Catal. Today Vol. 35 pp. 75-81.*

[12] Schimizu, K., Satsuma, A. and Hattori, T., 2000. Catalytic performance of $Ag-Al_2O_3$ catalyst for the selective catalytic reduction of NO by higher hydrocarbons. *Appl. Catal. B, Vol. 25 pp. 239-247.*

[13] Oscik, J., 1982. Adsorption,PWN-Polish Scientific Publishers Warszawa, page 41,page62.

[14] Kooten, W. E. J., Krijsen, H. C., Bleek, C. M. and Calis, H. P. A., 2000. Deactivation of zeolite catalysts used for NOx removal. *Appl. Catal. B, Vol. 25 pp. 125-135*.

[15] Ohtsuka, H. and Tabata, T., 2001. Roles of palladium and platinum in the selective catalytic reduction of nitrogen oxides by methane on palladium-platinum-loaded sulfated zirconia. *Appl. Catal. B, Vol. 29 pp. 177-183*.

[16] Shi, C., Cheng, M., Qu, Z., Yang, X. and Bao, X., 2002. On the selectively catalytic reduction of NOx with methane over Ag-ZSM-5 catalysts. *Appl. Catal. B, Vol. 36 pp. 173-182*.

[17] Zhu, Z., Liu, Z., Liu, S., Niu, H., Hu, T., Liu, T. and Xie, Y., 2000. NO reduction with NH3 over an activated carbon-supported cooper oxide catalysts at low temperatures. *Appl. Catal. B, Vol. 26 pp. 25-35*.

[18] Moreno-Tost, R., Castellon, E. R. and Jimenez-Lopez, A., 2006. Cobalt-iridium impregnated zirconium-doped mesoporous silica as catalysts for the selective catalytic reduction of NO with ammonia. *Jour. Molec. Catal. A Chem., Vol. 248 pp. 126-134*.

[19] Bassed, D. W. and Habgood, H. W., 1959. A gas chromatographic study of the catalytic isomerization of cyclopropane. *Jour. Phys. Chem., Vol. 64 pp. 769-773.*

[20] Topchieva, K. V., Romanovskii, B. V., Thoang, L. I. and Bizreh, Y. W. 1971. Procc. 4th Inter. Cong. Catal. 2, 135.

[21] Bizreh, Y. W. and Gates, B. C., 1984. Butane cracking catalyzed by the zeolite H-ZSM-5. *Jour. Catal., Vol. 88 pp. 240-243.*

[22] Girasimov, Y. and others, 1974. Physical Chemistry. *p.534.*

[23] Serra, R., Vecchietti, M. J., Miro, E. and Boix, A., 2008. In, Fe-zeolites: Active and stable catalysts for SCR of NOx-Kinetics, characterization and deactivation studies. *Catal. Today Vol. 133-135 pp. 480-486*.

[24] Winter, E. R. S. 1971. The catalytic decomposition of nitric oxide by metallic oxides. *J. Catalyst, V. 22, pp. 158-170*.

[25] Amirnazmi, A. Benson, J. E. and Boudart, M., 1973. Oxygen inhibition in the decomposition of NO on metal oxides and platinum. *J. Catalyst, V. 30, pp. 55-65.*